Automated Assessment of Pavement Rutting Using Mobile LiDAR Data

Ali Faisal
The University of British Columbia

Suliman Gargoum, Ph.D.
Assistant Professor
The University of British Columbia

Paper prepared for presentation at the Innovations in Pavement Management,
Engineering and Technologies Session

2023 TAC Conference & Exhibition, Ottawa, ON

Abstract

Pavement rutting is a common but critical form of deterioration in road surfaces that result in an uncomfortable ride for drivers while exposing them to potential safety risks including hydroplaning and loss of skid resistance. Transportation agencies periodically inspect and monitor road conditions for pavement distresses and plan rehabilitation procedures accordingly, but this routine process is labor-intensive, time-consuming, and prohibitively expensive. A significant amount of research was conducted to automate pavement crack detection, but this is not the case for equally important distresses such as permanent deformation. Efforts to automate rutting inspection processes were previously tackled using both pixel and point cloud methods. Cross-section pavement profiles are commonly used from mobile/terrestrial laser scans, and computational geometry techniques are employed to determine the rutting severity. However, only using cross-section profiles of the pavement rut and generating images from point cloud data may not provide a complete picture of the extent and degree of distresses across the entire pavement. To capture the complete surface geometry of the pavement and better assess road conditions, this research proposes a tile-based novel method for measuring and quantifying pavement rutting from LiDAR data by using road surface fitting and computational geometry algorithms. The effectiveness of this method is demonstrated through experiments on real-world pavement point cloud data. Overall, our method offers a fast and reliable way to measure pavement rutting using point clouds, delivering a more comprehensive view of pavement surface conditions compared to other methods. The ability to extract rutting information from point cloud pavement data is critical for entities looking to fully utilize mobile LiDAR datasets for pavement distress analysis to evaluate the condition of pavements and help determine the need for maintenance or rehabilitation.

Introduction

Permanent deformation, referred to as rutting, is one of the major distresses that severely deteriorate the performance of flexible pavements [1]. It is the longitudinal surface depression of the underlying layers along the wheel path, typically caused by repetitive traffic loads that incrementally accumulate permanent deformations over time [2]. The accumulation of ruts can seriously compromise the serviceability of roads by reducing the skid resistance, increasing the risk of hydroplaning, and overall increasing the maintenance cost of paved roads [3]. The issue is further exacerbated when accounting for the adverse effects that pavement rutting has on traffic safety [4]. As such, frequent road inspections and timely maintenance and rehabilitation operations become imperative to ensure that costs do not become prohibitively expensive otherwise and keep the roads a safer environment [4-5].

Inspection methods for rutting assessment and measurement are categorized into manual and automatic methods. Prior to the adoption of automated rutting data collection, the most commonly used manual method for rutting data collection was ASTM's Standard E1703M-10 "Straight Edge". To obtain a depth reading, a straight-edge object was placed on a lane covering the wheel path, and the vertical distance between it and the bottom of the rut was measured as illustrated in Fig. 1. Other manual methods included the rod and level method to measure the profile of a pavement by taking readings on the rod at different locations. At the Long-Term Pavement Performance Program (LTPP) test tracks, the Dipstick Road Profiler was used for transverse profile measurements by taking the difference in elevation between incremental distances along the wheel path [7-9].
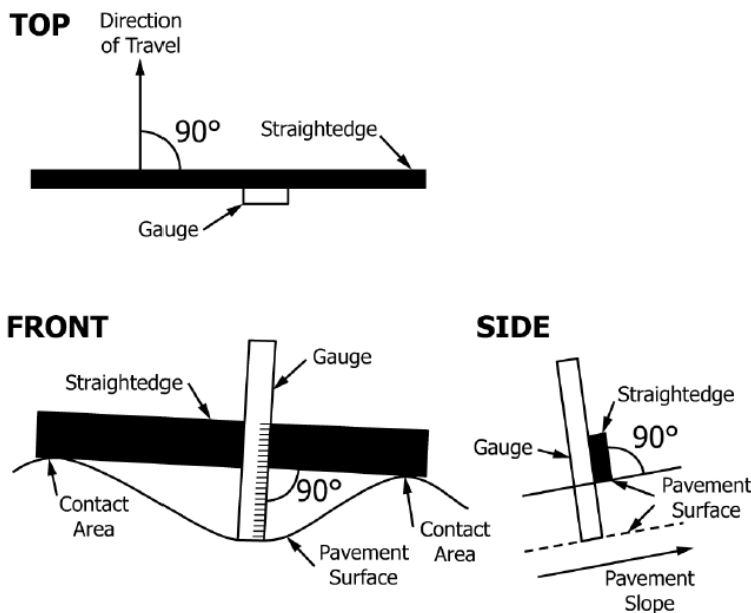

Fig. 1 Manual rut measurement using ASTM's straight-edge method *[6]*

While conventional methods do provide accurate rut depth measurements, they are subject to an inevitable amount of human error in the process, especially in harsh weather conditions or due to fatigue. This can lead to inaccuracies in rut depth readings resulting from either human error or shortcomings in the method. In addition, it becomes increasingly cumbersome when network-level rut assessments are needed and any disruption to the traffic flow is unfeasible. Besides that, these methods can be quite labor-intensive, slow, and places workers at risk of exposure to various hazards while on the road [9].

In the same way that road assessment technology is growing at an unprecedented rate, so have methods for evaluating and assessing rutting conditions in flexible pavements. New automatic methods cover a broad range of techniques and cross disciplines to capture the rutting performance of road networks such as image processing, 3D information obtained from Mobile Light Detection and Ranging (LiDAR) scans, non-contact profilometers, and machine/deep learning algorithms. LiDAR is a remote sensing technology that uses laser beams to measure distance and create high-resolution 3D maps of the scanned environment. The system works by emitting a pulsed laser beam and measuring the time it takes for the beam to return after hitting an object, which allows for the calculation of the object's distance and location. LiDAR is commonly used in various applications such as surveying, mapping, autonomous driving, and environmental monitoring. The main advantage of LiDAR over other techniques is its ability to capture the 3D representation of pavement surfaces which include elements such as pavement height, slope, and curvature. Besides that, LiDAR data can be collected quickly in large amounts at normal traffic speeds, and it can provide superior coverage of the pavement surface when compared to laser profilers. This can be particularly useful for continuously assessing pavement conditions over large areas or for identifying localized pavement distresses. This paper presents a novel technique for quantifying and evaluating pavement rutting by utilizing a tile-based approach with 3D LiDAR point cloud data of pavement surfaces. The proposed approach allows for accurate rut measurements that leverage the 3D feature of the road sections, allowing for more efficient and less costly pavement management and maintenance operations.

Literature Review

There is a growing potential in the ability to accurately detect and assess the rutting performance of road networks. Recent studies have leveraged the advancements in the field of computer vision and machine learning to find solutions for automating cumbersome pavement assessments. A study proposed an autonomous system that can measure pavement rutting by taking images using a high-speed shot camera while utilizing linear lasers to map the pavement surface and extract rutting values using common image processing techniques [10]. Hybridization of image processing techniques is more recently being used to improve the detection and accuracy of rutting assessments [11]. Moreover, other studies used rutting prediction models which generalize well given that sufficient data is available. For example, Shatnawi et al. [7] developed linear and non-linear regression models alongside an artificial neural network

(ANN). The latter was found to generalize better given a substantial number of road features were used.

Given the significant evolution of laser imaging technology in the last decade, several transportation agencies and scholars have adopted 3D data for the application of automated pavement distress data collection [12]. A recent study utilizing 3D images and deep learning developed an automated pavement distress detection framework using Faster Region-based Convolutional Neural Networks (Faster R-CNN) and the You Only Look Once (YOLO) v3 algorithm. Both techniques performed satisfactorily in detecting and classifying different crack types and potholes. While 625 3D images were annotated and labeled, the authors mentioned that the models could perform better when more images are used, especially for models similar to Faster R-CNN and architectures such as YOLO.

Recent studies started integrating LiDAR data into pavement assessment and monitoring operations since these scans can capture the pavement surface and the deviations within it [13]. In terms of pavement distress detection, one way to detect crack patterns in pavement point cloud scans was by using graph convolutional networks (GCN) and saliency-focused GCNs with dilated convolutions [14-15]. Other studies converted point clouds into images and applied processing techniques to filter, analyze and detect pavement cracks [16-17]. Zhong et al. also utilized popular image-based detection methods by processing point cloud data as images by using a time grid that contains the scan angle and acquisition time [18]. Georeferenced images were also generated from point clouds using a modified inverse distance weighted algorithm and cracks were extracted by tensor voting in the direction of nearby cracks [19]. Crack points can also be obtained from point clouds by using filtering algorithms based on elevation, intensity, and neighboring points [20-21]. Furthermore, road roughness can be estimated by applying Otsu thresholding to point cloud-generated intensity raster surfaces [22].

Despite the many different studies and frameworks that emerged to detect cracks in flexible pavements, the same can not be said regarding rutting assessments. One of the studies that attempted to detect rutting locations created a raster grid roadway surface from point clouds and used cell curvature to determine whether rutting at a specific location is present based on different thresholds [23]. El Issaoui et al. obtained rut profiles from Mobile Laser Scans (MLS) and the start, mid, and end points of the rut were obtained using a convex hull algorithm and k-means clustering. The rut depth was calculated as the difference between the tangent of these locations and a virtual linear surface [24]. Similarly, support points can be identified in rut profiles based on constraints such as not intersecting with the rut profile and the distance between these points set larger than the wheel path [25]. Gézero et al. introduced different strategies to extract cross-sections from point clouds to obtain the transverse profiles of the rut [26]. The canny edge detection algorithm was also used on digital surface models generated from point clouds to locate wheel paths and take transversal cross-sections to estimate rut depths [27]. Images were also obtained from point clouds so that elevation feature, slope feature, and aspect feature images can be constructed and assess rutting depths [28].

While the abovementioned methods have achieved satisfactory results in quantifying and evaluating pavement distress, the use of image-based methods has some limitations. For instance, deep learning models require copious amounts of labeled pavement images so that models can generalize well. Besides that, exterior factors such as lighting conditions, weather, and other low-quality images can significantly deteriorate the performance of the models [29]. Consequently, the task of image annotation is time-consuming, labor-intensive, and computationally expensive. In addition, rutting prediction models heavily depend on the availability of road feature data such as the road type, traffic volume, asphalt mix characteristics, and the number of rehabilitation, to name a few [8-12]. In addition, the use of MLS data for the estimation of rut depths is an active field of research. However, not only are there a limited number of studies, but the limited studies that do exist also typically rely merely on the cross-sectional information of the pavement. This is not completely representative of the 3D feature of the deformation since the location of where the cross section is taken plays a critical part in accurately estimating the rutting depth and the severity of the distress. In summary, the use of point clouds in pavement distress assessment produces rich road network data that can be captured at highway speeds and consequently eliminates road closures, putting workers at risk, and time-consuming inspections. To the best of the authors' knowledge, no study has yet attempted using LiDAR data for pavement rut assessment using the pavement's 3D feature characteristics, therefore, this paper proposes a novel method that assesses pavement rutting based on road tiles from MLS data.

Data Acquisition

Data used in this study was collected along Alberta Provincial Highway No. 32, commonly referred to as Highway 32. This north–south highway is located in west–central Alberta, Canada. It begins at its junction with Highway 33 in the Town of Swan Hills and proceeds south for 69 km where it meets Highway 43 northwest of Whitecourt. Due to the central location of the highway, regular inspection of pavement distresses is important for timely maintenance operations. The data was collected using the Leica Pegasus: Two Ultimate Laser Scanning System. The system has four built-in pavement cameras and two 360° spherical fish-eye cameras. In addition, the primary sensors of the system include a Global Navigation Satellite System (GNSS) and an inertia measurement unit (IMU). The system can produce dense 3D point clouds with spatial positioning data at vehicle operating speeds. The system is equipped with the ZF 9012 laser sensors, which can collect up to one million points per second with a relative accuracy of 1 mm. It is worth mentioning here that the relative accuracy is especially important in rutting estimation applications using 3D point clouds to ensure good uniformity in the data to be able to obtain the spatial information of the pavement that accurately represents the actual road surface topology.
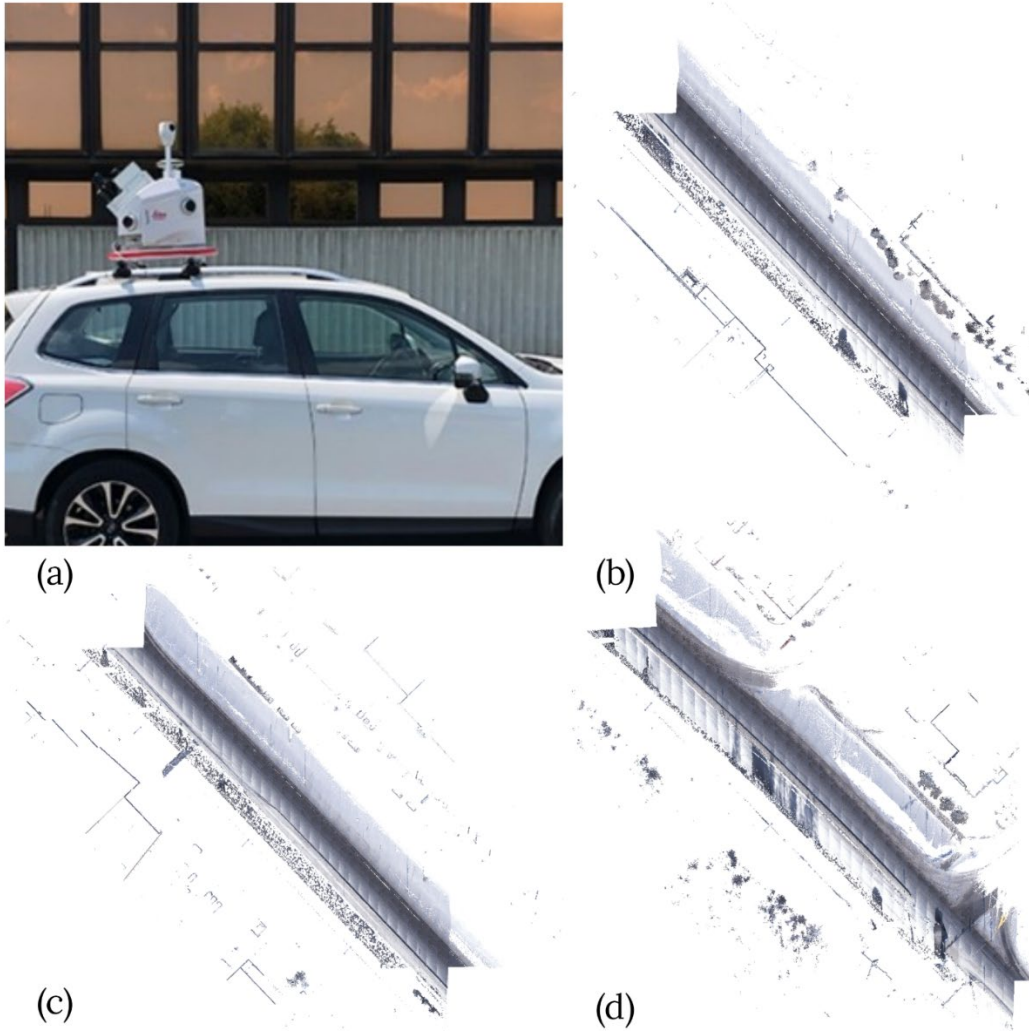
Fig. 2 Pavement point cloud data acquisition, (a) Leica Pegasus Two Ultimate, (b) road section 1; (c) road section 2; (d) road section 3

Point cloud datasets, depending on the scanned area, can get quite large in size, with increasingly computational intensity. As such, Highway 32 road segment was split into three road sections to lower the computational complexity of the analysis while retaining all information from the scans.

Characteristic of Pavement Point Clouds

Typically, road surfaces when paved with asphalt are compacted to flatten the pavement surface and minimize lateral variations along the longitudinal direction of the road. While some deformation might happen due to compressive forces from traffic loadings, that initial consolidation, if compaction was adequate, does not warrant a significant problem to the road serviceability and the pavement remains mostly flat. However, when rutting occurs, the pavement surface is no longer flat due to the accumulation of unrecoverable deformations in the semi-viscous asphalt state caused

by repetitive loading. In the context of point clouds, when there is no deformation along the pavement, the surface's profile is mostly flat, and the points belong to the same 3D plane. When rutting is present, point clouds reflect the spatial deformation that occurred along the road 3D pavement layer as seen in Fig. 3. In other words, the irregularities in the surface can be represented by points that deviate from the flat plane of the road. It can be observed that there is an abrupt change in the slope from the pavement to the rutting location, where the maximum value of deformation is located at the middle bottom region.

Since rutting points in the point cloud are irregularities in the road surface, the planar features of a road point cloud can be used. In general, planar features in point clouds refer to flat regions that can be used to approximate a plane, such as floors, walls, and ceilings. In the case of pavement surfaces, planar features can be used to identify the flat sections of the road and consequently the areas of deformation caused by rutting.
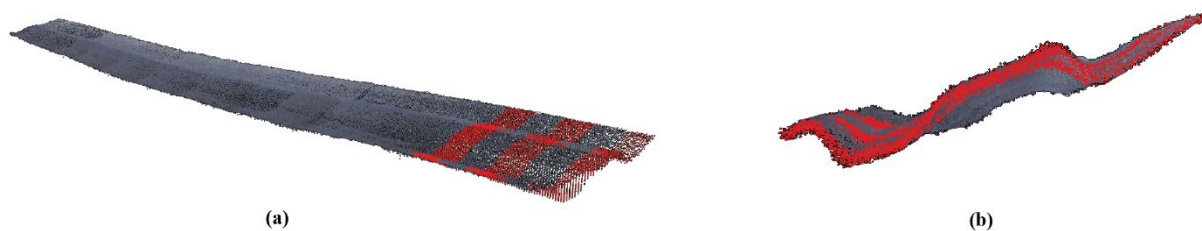

(a)   (b)

Fig. 3 Sample tiling of road surface point cloud with rutting along the wheel path. Linear road surface (left) and road cross-section (right)

Methodology

This section presents an overview of the algorithm proposed in this research. It involves several steps from extracting the pavement surface, preprocessing the data, creating boundaries, tiling the pavement surface, fitting 3D planes onto each tile and calculating the deviation from the plane to obtain rutting measurements. A summary of the proposed method is presented in Fig. 4. In the following sections, each step is explained in further detail.

Extraction of Road Surface

The generated raw 3D point cloud data of Highway 32 from the scan contains different types of structures other than the road such as buildings, trees, traffic signs, and other objects. The first step is to segment the objects of the point cloud and retain only points associated with the road surface. In this paper, point cloud segmentation was done using deep learning algorithms that work on classifying the point cloud into multiple features based on the availability of training data.
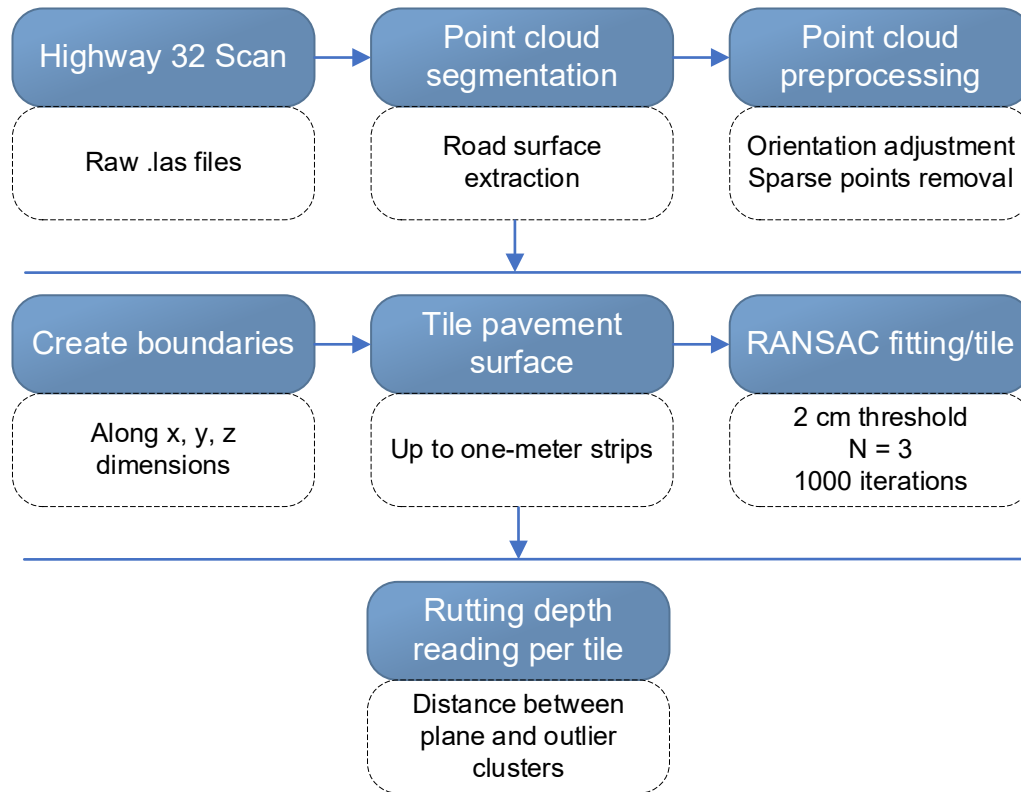
Fig. 4 Methodology flowchart

Point Cloud Preprocessing

After obtaining the road surface, the orientation of the road surface is adjusted. The orientation of point cloud data may not always be aligned with the direction of the road, especially if the data were obtained from different sources or angles. By adjusting the orientation around the z-axis by approximately 45 degrees, the x-axis and y-axis are made to represent the width and length of the road segment, respectively. This makes it easier and more convenient to analyze and visualize the data, especially when detecting rutting and pothole patterns along the length of the road is of importance.

Sparse points in raw point cloud datasets refer to points that have no neighboring points in close proximity. Removing sparse points from the road surface is particularly important to have an accurate representation of the actual road surface. Otherwise, they can lead to inaccuracies and errors in road condition analysis. For example, for the purposes of rutting measurements, these sparse points may lead to the underestimation or overestimation of rutting severity as any distance measurement would be altered by the random and isolated cluster locations of sparse points. To remove these points, different methods were used with varying success rates. The first approach was applying a density-based clustering algorithm (DBSCAN) that groups together points that are close to each other and separates points that are in areas of low density. In this implementation, the algorithm clusters the point cloud into road and non-road points. However, points that are part of the road were also removed since some areas along

the road do not have a very high point density, particularly at the edges. The same issue was also present in both the distance from the centroid, and grid-based noise removal methods. In addition to being computationally simple, sparse points were removed adequately using a k-nearest neighbor algorithm.

Pavement Surface Point Cloud Tiling

In many applications of point cloud processing, specifically when it comes to road surface analysis, it is often necessary to analyze large point cloud datasets covering the scanned area. However, processing the entire road surface can be computationally expensive, time-consuming, and can sometimes lead to memory limitations. In such cases, tiling the point clouds into smaller, more manageable sections can be an effective solution. Tiling the road surface involves dividing the road into smaller, overlapping square or rectangular regions called tiles. Once the road surface is tiled, each tile can then be processed individually and combined to generate a thorough analysis of the entire road surface.

Tiling the road surface provides a number of advantages over processing it as a single point cloud: (1) it can help reduce the computational cost by allowing parallel processing of individual tiles, making it easier to deal with smaller data sizes and complex structures, (2) it can facilitate the identification of smaller features in the terrain as the smaller sections make it more convenient to analyze, and (3) it provides an effective method to assess and characterize rutting in roadways since it allows for more precise and accurate measurement of numerous rutting regions. For example, tiling the point clouds for separate lanes and specific regions along the longitudinal direction of the pavement provides the ability to analyze certain locations of interest in greater detail and scrutiny. Unlike previous studies, the tiling approach proposed in this paper allows for localized pavement assessments by taking the entire 3D feature of each tiled pavement surface instead of assessing the rut depth based on transverse profiles.

For a point cloud $P = [p_1, p_2, \ldots, p_N]$ with N defined as the number of points, and $pi = [x_i, y_i, z_i]$ is a point in $\mathbb{R}^3$, the boundaries for the road surface are selected based on the coordinates of the minimum and maximum points in the x, y, z dimensions. The number of tiles in each dimension is then determined by dividing the tile size T by the bounds in each dimension to obtain T_x, T_y and T_z. The bounds of the i-th, j-th, and k-th tiles are then given by:

$$x_{minimum} = \min x + i * T \ where \ i = [0, 1, \ldots, T_{x-1}]$$

$$x_{maximum} = x_{minimum} + T$$

$$y_{minimum} = \min y + j * T \ where \ j = [0, 1, \ldots, T_{j-1}]$$

$$y_{maximum} = y_{minimum} + T \tag{1}$$

$$z_{minimum} = \min z + k * T \ where \ k = [0, 1, \ldots, T_{k-1}]$$

$$z_{maximum} = z_{minimum} + T$$

The set of points in a tile in the i-th, j-th, and k-th tile can be expressed as a set of points in M:

$$M \in P_n : n = 1, .., N, [x_{i,j,k} < x_n < x_{i,j,k+1}], [y_{i,j,k} < y_n < y_{i,j,k+1}], [z_{i,j,k} < z_n < z_{i,j,k+1}] \quad (2)$$

In eq (2), P_n represents a point in a point cloud P and $x_{i,j,k}$, $y_{i,j,k}$, $z_{i,j,k}$ are the lower and upper bounds of the coordinate values for a tile. The set M is created by iterating over all points in the point cloud P and selecting only those that lie within the tile or sub-region specified by the minimum and maximum coordinate values. Pavement tiles are then further processed by removing tiles that have a small number of points encompassed in them.

Tile Surface Fitting

The tiles of a road surface provide a way to represent the geometry of the pavement. Ideally, that surface would be flat or the lateral variations across each tile would be negligible in ideal road conditions. As the deformations accumulate due to traffic loading, part of the deformation is bounced back due to the viscoelasticity of asphalt, and part is permanently deformed. As such, any deviations from the flat surface can indicate the extent of the permanent deformation that occurred in the pavement. To determine the surface depression, a RANdom SAmple Consensus (RANSAC) approach can be used to fit each tile to a plane in 3D space since in any pavement tile, the majority of points are supposed to be flat while rutting includes a relatively less portion of the points.

RANSAC works iteratively for fitting models to data with outliers by randomly selecting a small subset of the data and using that subset to fit a model. Depending on the number of points that fit within the model, the process is repeated until sufficient points are fitted by a plane, or the maximum number of iterations is reached. The RANSAC algorithm was used iteratively to fit each tile of the pavement surface for each lane along the longitudinal direction.

Once a best-fit 3D plane has been identified for each tile of the road surface, the distance between the fitted plane and each outlier point can be computed. The distance of each outlier point that is below the plane and the fitted plane represents the height below the plane in the lateral direction. Therefore, for a given road tile, the maximum deviation of all points from the plane can represent the extent of rutting depth. The distance can be calculated as the mean lateral difference (perpendicular distance) between the group of outlier points and the plane.

Results and Discussion

To evaluate the performance of the proposed approach, point cloud datasets of three sections of Highway 32 were used. Each section represents a different type of highway configuration: section 1 is a two-lane undivided highway spanning 181 meters; Section 2 is a three-lane undivided highway with a length of 96 meters; and Section 3 is a 62-meter-long three-lane undivided highway featuring a left-turn lane at a signalized intersection.

The road sections were selected to test the proposed method on different lane functions as the traffic type, loading, and volume typically vary for each lane, and consequently, so would the strains and stresses imposed on the pavement. The number of calculated tiles for each road section was 226, 195, and 168 for road sections 1, 2, and 3, respectively. Each point cloud tile, representing a segment of a lane along the longitudinal direction of the road, was used to calculate the deviation in the lateral direction between the RANSAC-fitted tile and the anomalous data point that can be attributed to rutting at the pavement layer. The rut depths varied, depending on the road type and lane type, between 5.84 mm and 45.40 mm as shown in Fig. 5. The kernel density method in the violin plot shows the distribution of the rutting measurements, which demonstrate the degree of rutting for each lane and whether any extreme values are present.

For road section 1, the mean rut depth in the right lane is higher than in the left lane. In road section 2, the left lane had significantly less rutting than the other two lanes, while the mean rut depth in the left and right lanes in road section 3 is higher than the middle lane. It is worth mentioning that the rut depths in road section 3 in the right lane indicate that there might be a pothole or severely chipped aggregates from the pavement surface, so visual inspections of the site would be needed to further validate the distress in such cases and ensure that the proposed method was capable of capturing such conditions in the pavement.

Bituminous materials, such as asphalt binders commonly utilized in asphalt pavements, exhibit viscoelastoplastic properties that engender time- and temperature-dependent behavior. For instance, based on the time-temperature superposition principle [30], asphaltic materials behave akin to viscous materials under conditions of high temperatures, longer loading frequencies (i.e., slower speeds), or high loading magnitudes. This renders asphalt pavements more susceptible to permanent deformation and hence the prefix "visco" before "elastoplastic", where the asphalt mix loses some of its elastic properties and starts to deform irreversibly. In contrast, under opposite conditions, asphalt becomes more rigid and plastic and consequently more vulnerable to different types of distresses, such as fatigue, resulting from traffic loading, subbase structural problems, or weather conditions.

The proposed rutting measurement method is capable of capturing this behavior based on the calculated rut depths for each road section which are summarized in Fig. 6. In road section 1, the higher mean rut depths in the right lane can be attributed to several factors such as slower speeds, heavy trucks utilizing the right lane due to traffic regulations, and excessive braking and turning points to other destinations which would place stationary loads on the pavement surface. In contrast, rutting measurements in the left lane of road section 2 in Fig. 6(b) were substantially less than the other two lanes, which is a reasonable observation given that the left lane is typically used for higher speeds, which would lower the time that the pavement is under traffic loading.
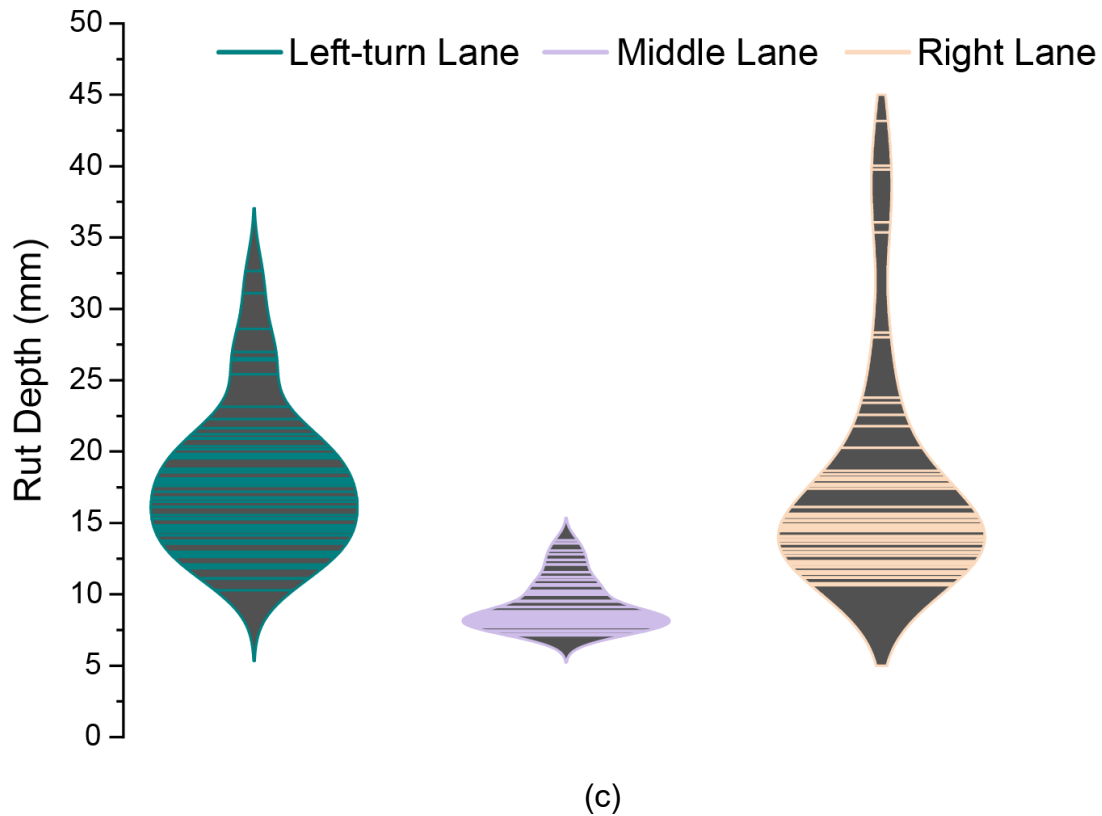
(a)

(b)

(c)
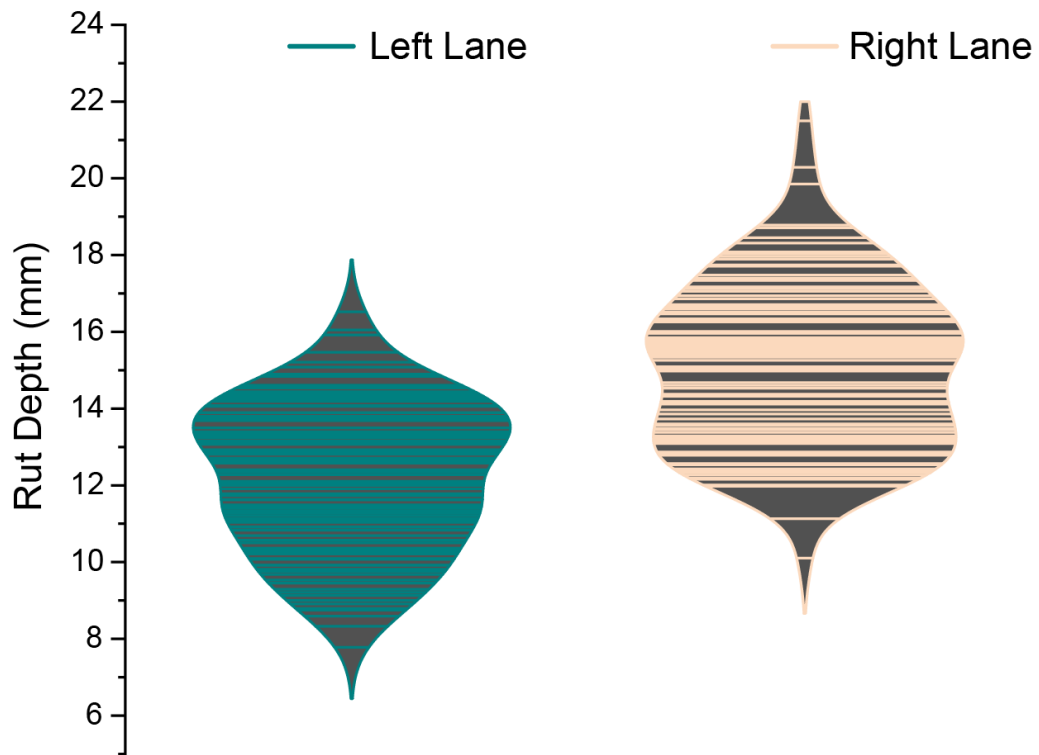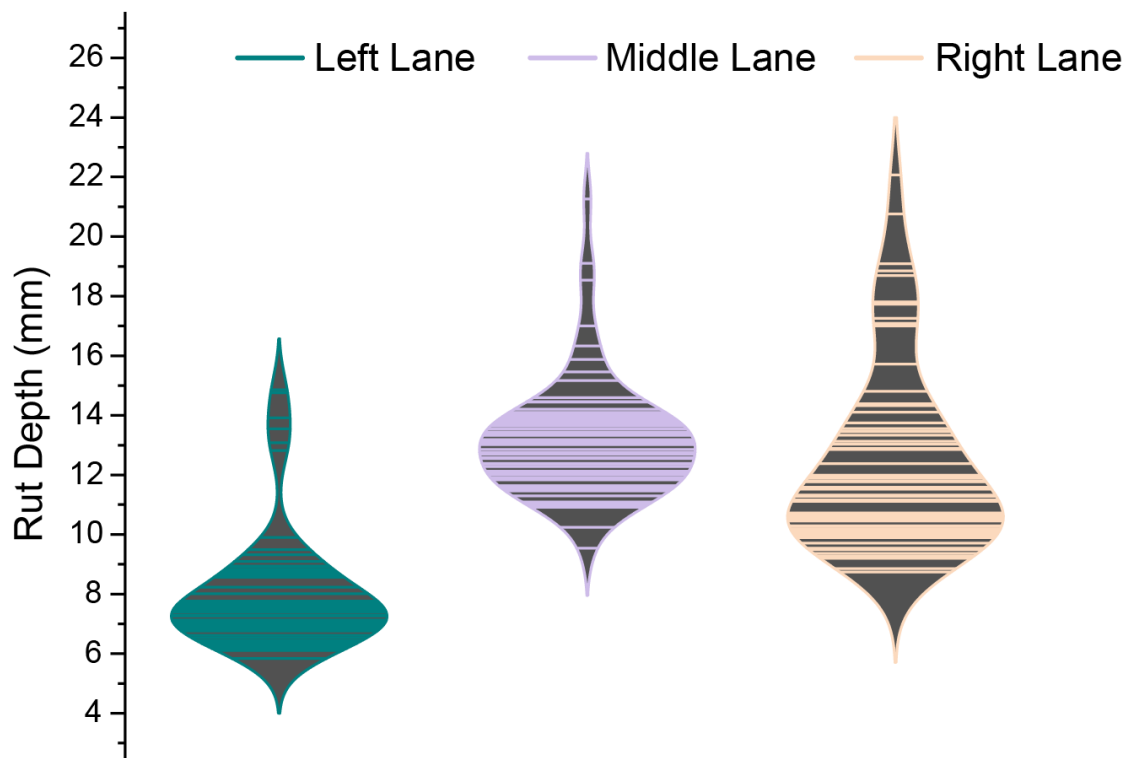
Fig. 5 Violin plots showing the distribution of rutting measurements in: (a) road section 1; (b) road section 2; (c) road section 3

As for road section 3, it includes a signalized intersection with a protected left-turn at the end of the road segment, so vehicles intending to turn left have to wait until the stop light permits. These stationary or slow-moving vehicles cause an increase in the time that the pavement is under loading, consequently leading to the accumulation of permanent deformations in the viscous asphalt condition and an inability for the deformation to partially recover after the load is removed [31]. While the same can be said about both the through and right lanes in an intersection, these traffic loadings might not be long enough to cause the same degree of damage to the pavement since the deformation can be partially recovered upon load removal under elastic/semi-elastic conditions.

The excessive rut depths depicted in Fig. 6(c) suggest the presence of underlying pavement failures in the queue box area at the end of the road segment. Further investigation is necessary to determine the cause of the abnormal rut measurements detected in these tile segments. A transversal profile analysis of the area can provide valuable insights into the nature of the deformation.
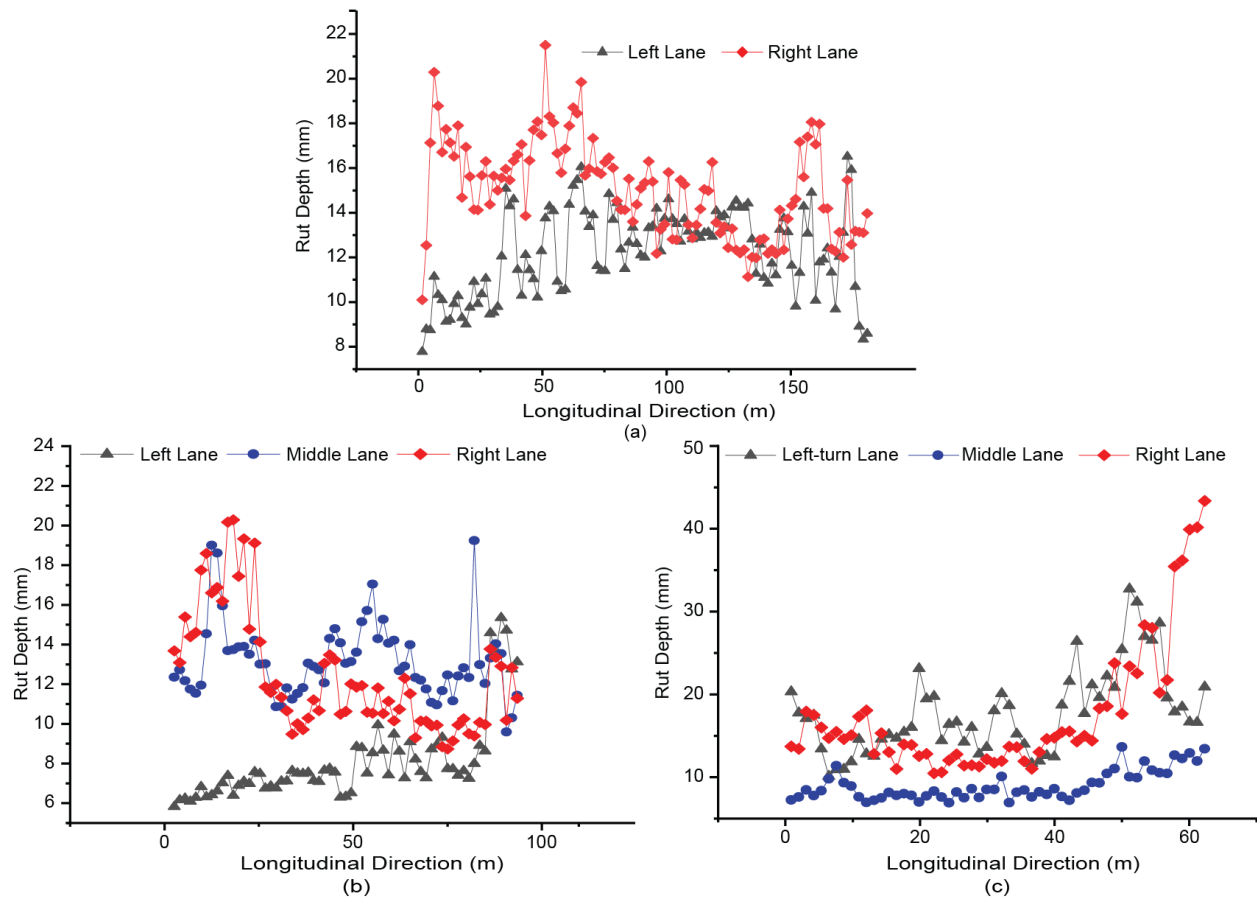
Fig. 6 Rutting depth along the longitudinal direction for each lane function: (a) 2-lane roadway; (b) 3-lane roadway; (c) 3-lane roadway with a left-turn lane in an intersection

As illustrated in Fig. 7, the transversal profile of the severely rutted region at the queue box reveals two main observations. Firstly, the extent of rutting shown in the profile supports the accuracy of the proposed methodology in presenting the degree of rutting in each 3D tile. Secondly, the distress is observed along both wheel paths, indicating that the pavement's severe rutting in this particular region is exacerbated by other pavement failure mechanisms. By inspecting the location of the road section using satellite imagery, shown in Fig. 8, it is apparent that the pavement has undergone significant deterioration and shows multiple distress types are present including potholes, alligator and thermal cracks, aggregate raveling, and severe rutting along the wheel path. These distress types are often indicative of underlying issues such as inadequate compaction during construction, improper asphalt mix design, and increased wear and tear due to heavy traffic. Additionally, environmental factors such as temperature fluctuations and precipitation may exacerbate the pavement distress, leading to further deterioration. The presence of asphalt bleeding also indicates that the binder has become too soft and is no longer providing the necessary support to the pavement structure.
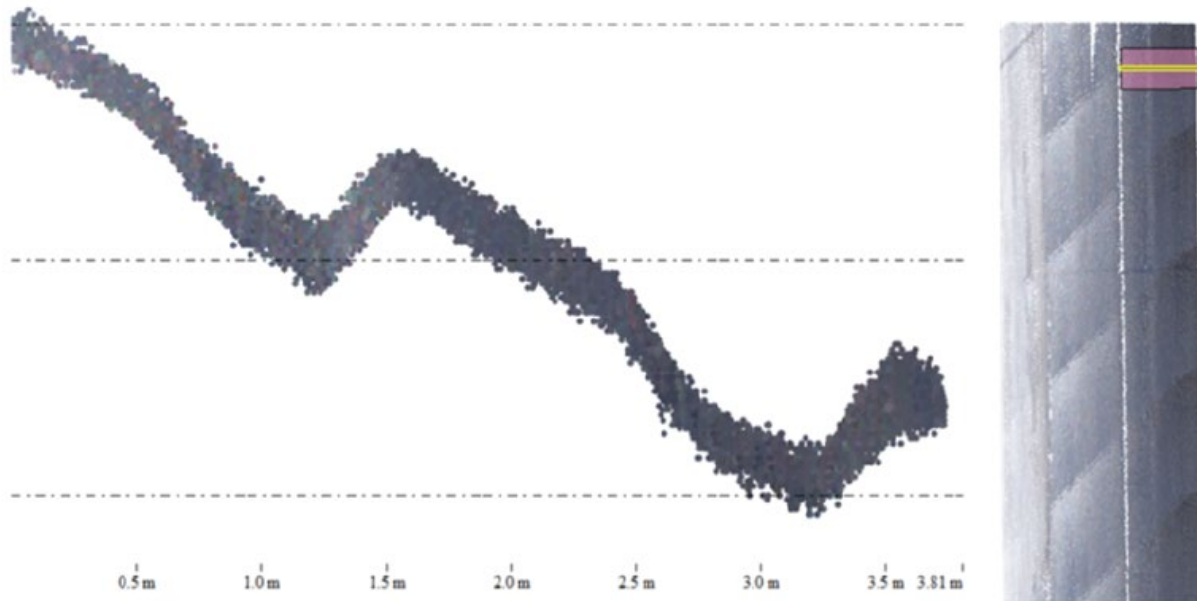
Fig. 7 Transversal profile of the region of interest identified by the proposed method

Fig. 8 Satellite imagery of the pavement condition [32]

The proposed method holds significant value as it aids in identifying regions with elevated levels of rutting, which could also indicate the presence of other pavement damage and potential safety hazards. The algorithm directly utilizes LiDAR data to assess the rutting depth in each pavement region without the need for expensive computational processing or rendering of 2D images. The runtime for the algorithm is less than 100 seconds for a total of 7-million-point density representing 339 meters of pavement surface. Compared to other methods that extracts rutting based on the conversion of LiDAR data to 2D images, digital terrain models, or use complex algorithms that operate on transformed variations of point clouds, the algorithm presented in this paper runs more efficiently due to its direct utilization of LiDAR data and tiling technique. The degree of rutting on each road tile for the three road sections is presented in the form of a heatmap in Fig. 9, providing essential information to plan maintenance and rehabilitation activities, such as resurfacing or strengthening the pavement structure. Furthermore, it also helps evaluate the efficiency of different

pavement materials and asphalt mix designs by analyzing the deformation levels at various highway locations. This facilitates determining which designs and materials offer acceptable rutting resistance to ensure a longer pavement service lifespan. The proposed method can also be used for monitoring pavement conditions over time. Regular scanning of roads of interest and calculating tile-based rutting measurements facilitate the tracking of changes within each section of the road, enabling timely interventions before they develop into costly issues. This can result in substantial savings in maintenance, rehabilitation, and labor costs, and increase road user safety.
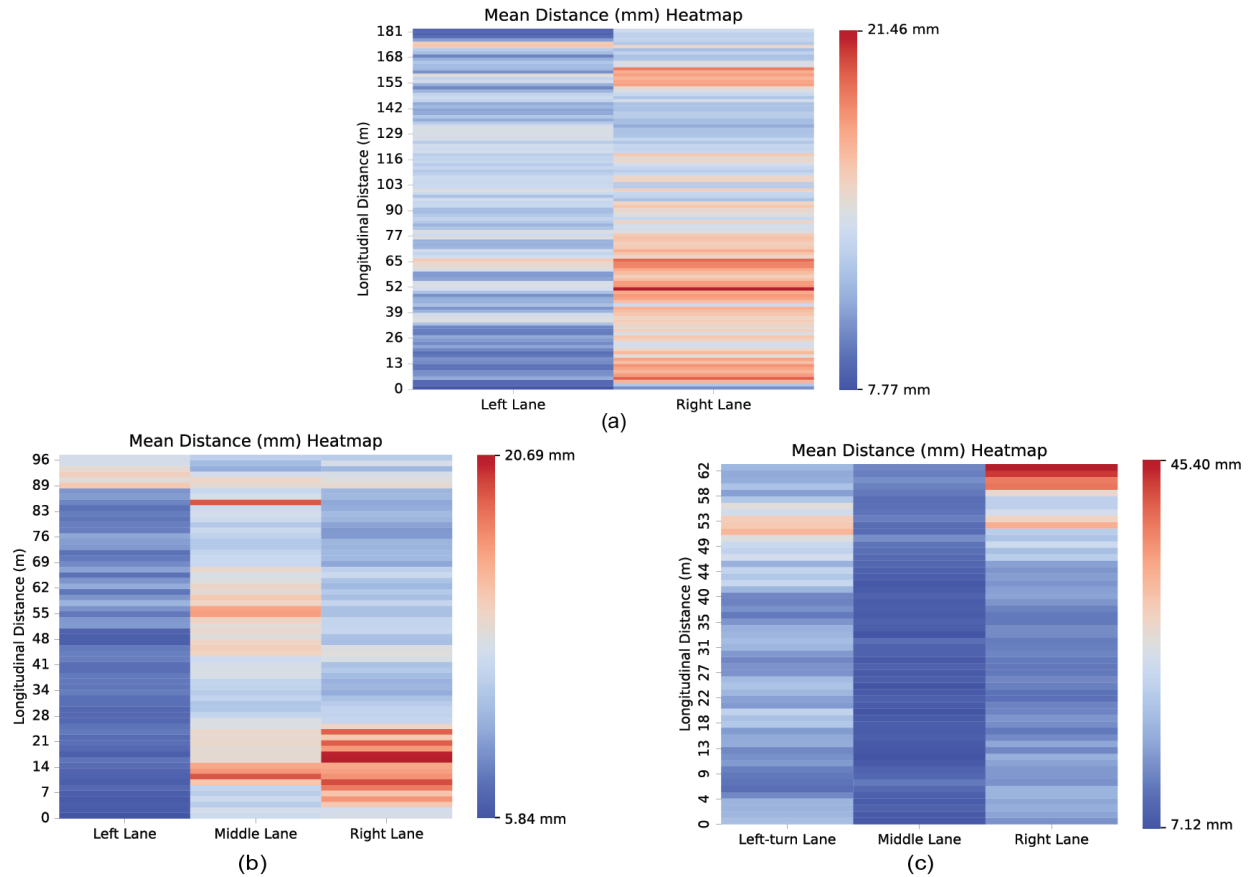

Fig. 9 Rutting severity heatmap for: (a) road section 1; (b) road section 2; (c) road section 3

Conclusion and Summary

In this paper, a tile-based rut estimation method was presented that involves tiling pavement surface point clouds into smaller, overlapping rectangular regions called tiles for each lane along the road longitudinal direction. In total, 181, 96, and 62 meters of pavement surface were used for road sections 1,2, and 3 respectively. Then, rut measurements for each tile were calculated based on the lateral distance between a fitted 3D plane between a tile and the points that are outside of the plane that follow the geometry of a pavement rut. By calculating the rut depth for each tile, an assessment of

rutting at various, user-defined regions along the length and lanes of the road can be conducted. The proposed method was capable of accurately presenting the degree of rutting along the pavement surface in the three tested road sections. The method was validated by comparing the computed rut measurements from the tiles and the transverse profiles of the regions. It is adequate for identifying locations of high rutting severity which may indicate the existence of other underlying pavement conditions. In particular, this approach can be especially valuable for transportation agencies when compared to other costly and time-consuming traditional pavement assessments, especially when network-level rut evaluation is required that other methods do not address by relying on transverse profiles for rut estimations.

Future research could explore the applicability of the proposed method in assessing pavement rutting when using more affordable LiDAR sensors with potentially lower point density than those employed in this study. The goal would be to evaluate the performance of scanning devices equipped with sensors that can provide a suitable scanning frequency while maintaining sufficient detail and accuracy in capturing rut shape and depth, even with reduced point density. Further research could assess the proposed methodology's applicability using LiDAR highway scans generated by low-cost sensors and explore its feasibility and practicality for pavement rutting assessment. The possibility of using low-cost LiDAR sensors in such applications can be extremely useful by increasing the accessibility of such techniques to transportation agencies and professionals in the field.

References

[1]   A. K. Singh and J. P. Sahoo, "Rutting prediction models for flexible pavement structures: A review of historical and recent developments," *Journal of Traffic and Transportation Engineering (English Edition)*, vol. 8, no. 3, pp. 315–338, Jun. 2021, doi: 10.1016/j.jtte.2021.04.003.

[2]   N. Chilukwa and R. Lungu, "Determination of Layers Responsible for Rutting Failure in a Pavement Structure," *Infrastructures*, vol. 4, no. 2, Art. no. 2, Jun. 2019, doi: 10.3390/infrastructures4020029.

[3]   T. F. Fwa, H. R. Pasindu, and G. P. Ong, "Critical Rut Depth for Pavement Maintenance Based on Vehicle Skidding and Hydroplaning Consideration," *Journal of Transportation Engineering*, vol. 138, no. 4, pp. 423–429, Apr. 2012, doi: 10.1061/(ASCE)TE.1943-5436.0000336.

[4]   Ahmed Samah Shyaa and Ir Dr Raha Abd Rahma, "Review: Asphalt Pavement Rutting Distress and Affects on Traffics Safety," *JTTE*, vol. 10, no. 1, Feb. 2022, doi: 10.17265/2328-2142/2022.01.004.

[5]   A. Shtayat, S. Moridpour, B. Best, A. Shroff, and D. Raol, "A review of monitoring systems of pavement condition in paved and unpaved roads," *Journal of Traffic and Transportation Engineering (English Edition)*, vol. 7, no. 5, pp. 629–638, Oct. 2020, doi: 10.1016/j.jtte.2020.03.004.

[6]   ASTM 1703/E 1703M, "Test Method for Measuring Rut-Depth of Pavement Surfaces Using a Straightedge," ASTM International. doi: 10.1520/E1703_E1703M-10R23.

[7]   N. Shatnawi, M. Taleb Obaidat, and A. Al-Sharideah, "Modeling Road Pavement Rutting Using Artificial Neural Network and Conventional Measurements," *Transportation Research Record*, p. 036119812211102, Jul. 2022, doi: 10.1177/03611981221110224.

[8]   R. W. Perera, S. D. Kohn, and G. R. Rada, "Long-Term Pavement Performance Program Manual for Profile Measurements and Processing," *No. FHWA-HRT-08-056. Turner-Fairbank Highway Research Center, McLean, VA*, 2008.

[9]   P. A. Serigos, J. A. Prozzi, B. H. Nam, and M. R. Murphy, "Field Evaluation of Automated Rutting Measuring Equipment," *No. FHWA/TX-12/0-6663-1 Center for Transportation Research, The University of Texas, Austin*, 2012.

[10]   S. Arezoumand, A. Mahmoudzadeh, A. Golroo, and B. Mojaradi, "Automatic pavement rutting measurement by fusing a high speed-shot camera and a linear laser," *Construction and Building Materials*, vol. 283, p. 122668, May 2021, doi: 10.1016/j.conbuildmat.2021.122668.

[11]   M.-T. Cao, K.-T. Chang, N.-M. Nguyen, V.-D. Tran, X.-L. Tran, and N.-D. Hoang, "Image processing-based automatic detection of asphalt pavement rutting using a novel metaheuristic optimized machine learning approach," *Soft Comput*, vol. 25, no. 20, pp. 12839–12855, Oct. 2021, doi: 10.1007/s00500-021-06086-5.

[12]   K. C. P. Wang and O. Smadi, *Transportation Research Circular E-C156: Automated Imaging Technologies for Pavement Distress Surveys*. Washington, D.C.: Transportation Research Board, 2011, p. 22866. doi: 10.17226/22866.

[13]   S. Gargoum and K. El-Basyouny, "Automated extraction of road features using LiDAR data: A review of LiDAR applications in transportation," in *2017 4th International Conference on Transportation Information and Safety (ICTIS)*, Banff, AB, Canada: IEEE, Aug. 2017, pp. 563–574. doi: 10.1109/ICTIS.2017.8047822.

[14]   L. Ma and J. Li, "SD-GCN: Saliency-based dilated graph convolution network for pavement crack extraction from 3D point clouds," *International Journal of Applied Earth Observation and Geoinformation*, vol. 111, p. 102836, Jul. 2022, doi: 10.1016/j.jag.2022.102836.

[15]   H. Feng *et al.*, "GCN-Based Pavement Crack Detection Using Mobile LiDAR Point Clouds," *IEEE Transactions on Intelligent Transportation Systems*, vol. 23, no. 8, pp. 11052–11061, Aug. 2022, doi: 10.1109/TITS.2021.3099023.

[16]   X. Xu and H. Yang, "Intelligent crack extraction and analysis for tunnel structures with terrestrial laser scanning measurement," *Advances in Mechanical Engineering*, vol. 11, no. 9, p. 168781401987265, Sep. 2019, doi: 10.1177/1687814019872650.

[17]   W. Zhu, W. Tan, L. Ma, D. Zhang, J. Li, and M. A. Chapman, "A Capsnets Approach to Pavement Crack Detection Using Mobile Laser Scannning Point Clouds," in *The International Archives of Photogrammetry, Remote Sensing and Spatial Information Sciences*, Gottingen, Germany: Copernicus GmbH, 2021, pp. 39–44. doi: 10.5194/isprs-archives-XLIII-B1-2021-39-2021.

[18]   M. Zhong, L. Sui, Z. Wang, and D. Hu, "Pavement Crack Detection from Mobile Laser Scanning Point Clouds Using a Time Grid," *Sensors (Basel)*, vol. 20, no. 15, p. 4198, Jul. 2020, doi: 10.3390/s20154198.

[19]   H. Guan *et al.*, "Iterative Tensor Voting for Pavement Crack Extraction Using Mobile Laser Scanning Data," *IEEE Transactions on Geoscience and Remote Sensing*, vol. 53, no. 3, pp. 1527–1537, Mar. 2015, doi: 10.1109/TGRS.2014.2344714.

[20]   A. T. T. Phan and T. N. Huynh, "Pavement Crack Extraction Method from Mobile Laser Scanning Point Cloud," *Advances in Civil Engineering*, vol. 2022, p. e6317008, Jul. 2022, doi: 10.1155/2022/6317008.

[21]   Yongtao Yu, J. Li, Haiyan Guan, and Cheng Wang, "3D crack skeleton extraction from mobile LiDAR point clouds," in *2014 IEEE Geoscience and Remote Sensing*

Symposium, Quebec City, QC: IEEE, Jul. 2014, pp. 914–917. doi: 10.1109/IGARSS.2014.6946574.

[22]   P. Kumar and E. Angelats, "AN AUTOMATED ROAD ROUGHNESS DETECTION FROM MOBILE LASER SCANNING DATA," *Int. Arch. Photogramm. Remote Sens. Spatial Inf. Sci.*, vol. XLII-1/W1, pp. 91–96, May 2017, doi: 10.5194/isprs-archives-XLII-1-W1-91-2017.

[23]   A. Famili, W. A. Sarasua, A. Shams, W. J. Davis, and J. H. Ogle, "Application of Mobile Terrestrial LiDAR Scanning Systems for Identification of Potential Pavement Rutting Locations," *Transportation Research Record*, vol. 2675, no. 9, pp. 1063–1075, Sep. 2021, doi: 10.1177/03611981211005777.

[24]   A. El Issaoui *et al.*, "Feasibility of Mobile Laser Scanning towards Operational Accurate Road Rut Depth Measurements," *Sensors*, vol. 21, no. 4, p. 1180, Feb. 2021, doi: 10.3390/s21041180.

[25]   S. Firoozi Yeganeh, A. Golroo, and M. R. Jahanshahi, "Automated Rutting Measurement Using an Inexpensive RGB-D Sensor Fusion Approach," *Journal of Transportation Engineering, Part B: Pavements*, vol. 145, no. 1, p. 04018061, Mar. 2019, doi: 10.1061/JPEODX.0000095.

[26]   L. Gézero, C. Antunes, and this link will open in a new window Link to external site, "Road Rutting Measurement Using Mobile LiDAR Systems Point Cloud," *ISPRS International Journal of Geo-Information*, vol. 8, no. 9, p. 404, 2019, doi: 10.3390/ijgi8090404.

[27]   N. Shatnawi, M. T. Obaidat, and B. Al-Mistarehi, "Road pavement rut detection using mobile and static terrestrial laser scanning," *Appl Geomat*, vol. 13, no. 4, pp. 901–911, Dec. 2021, doi: 10.1007/s12518-021-00400-4.

[28]   R. Liu, H. Ren, Y. Chai, and J. Yang, "3D Rutting Features Extraction Through Continuous Pavement Laser Point Cloud," *Int. J. Pavement Res. Technol.*, Aug. 2022, doi: 10.1007/s42947-022-00193-8.

[29]   P. K. Saha, D. Arya, A. Kumar, H. Maeda, and Y. Sekimoto, "Road Rutting Detection using Deep Learning on Images," in *2022 IEEE International Conference on Big Data (Big Data)*, Dec. 2022, pp. 6507–6515. doi: 10.1109/BigData55660.2022.10020642.

[30]   Y. Zhao and Y. Richard Kim, "Time–Temperature Superposition for Asphalt Mixtures with Growing Damage and Permanent Deformation in Compression," *Transportation Research Record*, vol. 1832, no. 1, pp. 161–172, Jan. 2003, doi: 10.3141/1832-20.

[31]   X. Ji, N. Zheng, S. Niu, S. Meng, and Q. Xu, "Development of a rutting prediction model for asphalt pavements with the use of an accelerated loading facility," *Road*

Materials and Pavement Design, vol. 17, no. 1, pp. 15–31, Jan. 2016, doi: 10.1080/14680629.2015.1055337.

[32]   Google, "Google Maps location showing the pavement condition at queue box," 2023. Accessed: Apr. 21, 2023. [Online]. Available: https://goo.gl/maps/bbeZft1r2pp4Ujmr6